

Published in final edited form as:

AJR Am J Roentgenol. 2012 December ; 199(6): 1266–1274. doi:10.2214/AJR.12.9382.

Abdominal CT With Model-Based Iterative Reconstruction (MBIR): Initial Results of a Prospective Trial Comparing Ultralow-Dose With Standard-Dose Imaging

Perry J. Pickhardt¹, Meghan G. Lubner¹, David H. Kim¹, Jie Tang², Julie A. Ruma¹, Alejandro Muñoz del Río¹, and Guang-Hong Chen^{1,2}

¹Department of Radiology, University of Wisconsin School of Medicine and Public Health, E3/311 Clinical Science Center, 600 Highland Ave, Madison, WI 53792-3252

²Department of Medical Physics, University of Wisconsin School of Medicine and Public Health, Madison, WI

Abstract

OBJECTIVE—The purpose of this study was to report preliminary results of an ongoing prospective trial of ultralow-dose abdominal MDCT.

SUBJECTS AND METHODS—Imaging with standard-dose contrast-enhanced ($n = 21$) and unenhanced ($n = 24$) clinical abdominal MDCT protocols was immediately followed by ultralow-dose imaging of a matched series of 45 consecutively registered adults (mean age, 57.9 years; mean body mass index, 28.5). The ultralow-dose images were reconstructed with filtered back projection (FBP), adaptive statistical iterative reconstruction (ASIR), and model-based iterative reconstruction (MBIR). Standard-dose series were reconstructed with FBP (reference standard). Image noise was measured at multiple predefined sites. Two blinded abdominal radiologists interpreted randomly presented ultralow-dose images for multilevel subjective image quality (5-point scale) and depiction of organ-based focal lesions.

RESULTS—Mean dose reduction relative to the standard series was 74% (median, 78%; range, 57–88%; mean effective dose, 1.90 mSv). Mean multiorgan image noise for low-dose MBIR was 14.7 ± 2.6 HU, significantly lower than standard-dose FBP (28.9 ± 9.9 HU), low-dose FBP (59.2 ± 23.3 HU), and ASIR (45.6 ± 14.1 HU) ($p < 0.001$). The mean subjective image quality score for low-dose MBIR (3.0 ± 0.5) was significantly higher than for low-dose FBP (1.6 ± 0.7) and ASIR (1.8 ± 0.7) ($p < 0.001$). Readers identified 213 focal noncalcific lesions with standard-dose FBP. Pooled lesion detection was higher for low-dose MBIR (79.3% [169/213]) compared with low-dose FBP (66.2% [141/213]) and ASIR (62.0% [132/213]) ($p < 0.05$).

CONCLUSION—MBIR shows great potential for substantially reducing radiation doses at routine abdominal CT. Both FBP and ASIR are limited in this regard owing to reduced image quality and diagnostic capability. Further investigation is needed to determine the optimal dose level for MBIR that maintains adequate diagnostic performance. In general, objective and subjective image quality measurements do not necessarily correlate with diagnostic performance at ultralow-dose CT.

Keywords

adaptive statistical iterative reconstruction (ASIR); CT; dose reduction; low-dose CT radiation; model-based iterative reconstruction (MBIR)

Dose reduction in body CT has become a top priority because of concerns over the risks related to ionizing radiation [1, 2]. Dose reduction, however, must be balanced by an acceptable level of image quality, and above all, diagnostic accuracy must be adequately maintained. Although a variety of dose reduction strategies have been tested and implemented, perhaps most promising are the novel iterative reconstruction algorithms that have evolved beyond the traditional reconstruction method of filtered back projection (FBP) [3–10]. Adaptive statistical iterative reconstruction (ASIR) has been the most studied algorithm to date, yielding the possibility for estimated dose reduction in the range of 25–40% [4, 6, 8, 10]. The published research to date has largely focused on modest dose reductions of less than 50%, mainly in the evaluation of image noise and subjective image quality without formal evaluation of diagnostic accuracy [11]. In general, concurrent standard-dose imaging was not performed for direct comparison in these studies.

Model-based iterative reconstruction (MBIR), a version of which (Veo, GE Healthcare) was approved by the U.S. Food and Drug Administration (FDA) in September 2011, is a promising advance beyond ASIR and other available iterative methods. As the first true model-based reconstruction method in CT, MBIR has the potential to substantially reduce dose while improving resolution. To evaluate the feasibility of ultralow-dose body CT with MBIR and other novel reconstruction methods, we are conducting a prospective clinical trial whereby a series of ultralow-dose images, initially targeted at 70–90% dose reduction, is obtained immediately after routine clinical standard-dose imaging for direct side-by-side comparison of image quality and diagnostic utility. We report on our preliminary experience with ultralow-dose abdominal CT performed with MBIR and ASIR including comparison with ultralow-dose and standard-dose FBP reconstruction.

Subjects and Methods

Study Population and CT Protocol

This HIPAA-compliant prospective trial was approved by the institutional review board at our institution. All subjects provided signed informed consent. Patients eligible for inclusion in this ongoing study were men and nonpregnant women in whose care a decision had been made to proceed with abdominal CT evaluation at our institution. Routine CT protocols that qualified for study inclusion were unenhanced supine abdominal series and IV contrast-enhanced series in the portal venous phase. All studies were performed with a 64-MDCT scanner (Discovery CT750 HD, GE Healthcare) with collimated slice thickness at the isocenter of 0.625 mm, 120 kVp, tube current modulation (Smart mA, GE Healthcare), and a study-specific noise index, ranging up to 50 for the standard-dose series (Appendix 1). Of note, our current standard-dose protocols for the scanner used in this study are based on use of a 40% ASIR blend for clinical interpretation. Therefore, the percentage dose reductions seen with the ultralow-dose series are underestimated compared with those seen with use of older, traditional FBP protocols for the standard dose.

Immediately after the routine standard-dose abdominal CT acquisition, an ultralow-dose abdominal series was obtained with matching coverage with targeted dose reduction in the range of 70–90% based on the projected dose-length product from the clinical series. The tube current range, noise index, and associated slice thickness for acquisition were adjusted to achieve the targeted level of dose reduction. For IV contrast-enhanced studies, the

ultralow-dose series was obtained during the same breath-hold with image acquisition in the opposite table direction to minimize differences in phase of contrast enhancement. Contrast-enhanced images were obtained during the standard portal venous phase with iodinated nonionic contrast material and a saline chaser according to routine.

The ultimate recruitment goal for this large ongoing prospective trial is up to 500 subjects with a subsequent plan for more dedicated evaluation according to specific study indication (e.g., oncologic staging, urolithiasis, colonography). Herein we report the cumulative interim results with MBIR for imaging of the initial 45 subjects (24 men, 21 women; mean age, 57.9 years), pooling the IV contrast-enhanced CT cohort ($n = 21$) with the unenhanced CT cohort ($n = 24$). The mean body mass index was 28.5 (range, 19.4–41.6). Seventeen (37.8%) subjects were obese (body mass index > 30.0). The volume CT dose index $CTDI_{vol}$ (milligrays) and dose-length product (milligrays \times centimeters) were recorded for the matching standard-dose and low-dose series to establish the level of dose reduction (Table 1). The effective dose (millisieverts) was obtained from the dose-length product by use of the conversion factor of 0.015 mSv/(mGy \times cm) recommended by the American Association of Physicists in Medicine [12] and verified by Deak et al. [13].

CT Image Reconstruction

For the purposes of this study, the standard-dose abdominal CT series was reconstructed with the traditional FBP method to serve as the reference standard. Although our standard-dose protocols are based on a 40% ASIR approach, we chose not to use ASIR for the standard-dose reconstruction algorithm because FBP remains the dominant technique in use today and is not vendor specific and because most clinical scanners do not have ASIR capability. The accompanying ultralow-dose series was reconstructed with FBP, ASIR (ASiR, GE Healthcare), and MBIR for interpretation by blinded readers. For the ASIR series, a 40% blend was used to optimize subjective image quality, as previously described [4–6]. MBIR images were obtained with the FDA-approved version (Veo, GE Healthcare). All images (standard and low dose) were reconstructed with 2.5-mm slice thickness at 1.25-mm intervals in both the transverse (axial) and coronal planes.

CT Image Analysis

The CT images were systematically analyzed for image noise, subjective image quality, and depiction of focal lesions. For all series, image noise, reflected by the SD of attenuation (CT number in HU), was obtained in a 250-mm² circular region of interest (ROI). The ROI was placed in four standard locations: right hepatic lobe, left renal parenchyma, right paraspinous musculature, and left flank subcutaneous fat. ROI placement per patient for the low-dose series was exact because the ROIs were derived from the same dataset. ROI placement on the standard-dose series was matched as closely as possible to that on the ultralow-dose series (Fig. 1).

For assessment of diagnostic accuracy, focal organ-based lesion detection was undertaken by two fellowship-trained abdominal radiologists, each with extensive experience (18 and 8 years) reading body CT images, including images reconstructed with both FBP and ASIR. All ultralow-dose series (FBP, ASIR, and MBIR) for each patient (identifying information removed) were independently reviewed by blinded readers (without consensus) such that all images from the 45 cases, consisting of a random mix of the three reconstruction algorithms, were sequentially read in separate individual sessions by each reader (Figs. 1 and 2). A minimum washout period of 3 days was instituted at the end of each reading session to reduce recall bias between the four reading sessions. In most if not all cases, the interval between viewings of images of the same patient was at least 1 week. After all three randomized ultralow-dose series were interpreted for each patient, the standard-dose FBP

series for each patient was evaluated for focal lesions to serve as the clinical reference standard. Noncalcific focal lesions for the purpose of this preliminary study were defined and categorized as detectable organ-based foci larger than 3 mm involving the liver, pancreas, or kidneys. Focal noncalcified lesions could be of either increased or decreased attenuation relative to the organ containing them. Up to seven focal lesions per organ were counted and tabulated. Focal calcifications were not included in this analysis. Individual and pooled lesion detection for each low-dose series was compared against the standard-dose FBP reference standard and with the other ultralow-dose reconstructions.

To evaluate subjective image quality, four predetermined levels were graded for each case by the two reviewers (for a total of 32 subjective scores per patient). The following established 5-point scale was used: 0, nondiagnostic; 1, severe artifact with low confidence; 2, moderate artifact with moderate diagnostic confidence; 3, mild artifact with high confidence; 4, well depicted without artifacts [5]. To improve discrimination, 0.5-interval scores were allowed (e.g., 3.5). For the purposes of this study, we used a cutoff between 2.5 and 3.0 to differentiate unacceptable from acceptable image quality. Because we also included formal image interpretation for assessment of diagnostic performance, to avoid confusion and unnecessary complexity, we chose not to have separate subjective scores for both artifacts and diagnostic confidence. In each case, the two readers were blinded to reconstruction type for the ultralow-dose series (FBP, ASIR, and MBIR), and the reconstruction type was randomized for review. A score was derived for axial and coronal images with a soft-tissue window setting (width, 400 HU; level, 50 HU) on a standard PACS system. The four predetermined levels for scoring were through the portal vein bifurcation and sacroiliac joints for the axial images and through the kidneys and main portal vein for the coronal images (Fig. 3).

Statistical Analysis

Linear mixed-effects models were used to assess differences between reconstruction methods. These models take into account the correlation arising from the use of multiple reconstructions of multiple structures or tissues in the same subject. The models were fitted by maximum likelihood, and an independence working correlation structure was used. Separate models were fitted to each of the two readers. Adjusted Wald 95% CIs were obtained as appropriate. This analysis was performed separately for each reader and for their pooled data. Disjointedness (nonoverlap) of two 95% CIs was taken to represent statistically significant differences at the 5% level.

For assessment and comparison of diagnostic performance, the primary endpoint was pooled detection of focal, noncalcific organ-based lesions on the ultralow-dose series relative to the pooled detection on the standard-dose FBP series. Lesion-by-lesion matching results were not included in this initial analysis.

A value of $p < 0.05$ (two-sided) was the criterion for statistical significance. Residual and exploratory plots were obtained to assess possible violations in test assumptions. All statistical analysis and graphics were generated with R 2.12.1 software (R Development Core Foundation, 2009).

Results

The level of dose reduction compared with the standard-dose clinical series and the effective doses for the ultralow-dose series for each patient are shown in Table 1. The mean and median dose reductions for the entire group were 74% and 78% (range, 57–88%). These reductions were blunted somewhat by the use of ASIR-driven protocols for the standard-dose series and would have been greater if traditional FBP-driven protocols had been used.

The volume CT dose indexes for the standard-dose and low-dose series for each patient also are shown in Table 1. The mean and median effective doses for all ultralow-dose studies combined were 1.90 and 1.11 mSv. The mean effective doses for IV contrast-enhanced and unenhanced studies were 3.06 and 0.89 mSv. Not surprisingly, the effective doses were generally higher for the IV contrast-enhanced studies in larger patients (Appendix 1). Given the lower starting point for standard unenhanced CT studies and the ability to further decrease dose for indications for unenhanced imaging (i.e., colonography and urolithiasis evaluation), 19 of 24 (79.2%) unenhanced series had an effective dose of less than 1.0 mSv; only three contrast-enhanced series had a dose less than 1.0 mSv.

Mean image noise data for the four predefined anatomic locations are summarized in Table 2 according to the specific CT technique (with or without contrast enhancement) and image reconstruction method. The overall results are displayed graphically in Figure 4A. Overall, the mean image noise for MBIR (14.7 ± 2.6 HU) was significantly lower than for standard-dose FBP (28.9 ± 9.9 HU), low-dose FBP (59.2 ± 23.3 HU), and ASIR (45.6 ± 14.1 HU) ($p < 0.001$). Differences in measured image noise correlated well with the visual appearance (Fig. 1). MBIR image noise not only was three to four times lower than the corresponding low-dose FBP and low-dose ASIR image noise but also was significantly lower than the standard-dose FBP image noise ($p < 0.001$). Noise differences between the MBIR series and other series were even more pronounced on the unenhanced CT studies (Table 2). The overall mean noise difference between enhanced and unenhanced MBIR series was only 1 HU; this difference was greater for the other reconstruction methods.

Table 3 shows the summarized results for subjective image quality assessment by the two blinded reviewers. These results are combined graphically in Figure 4B. According to the 5-point quality score (0–4), the mean subjective image quality score at all four levels pooled between the two readers was significantly higher for low-dose MBIR (3.0 ± 0.5) than for low-dose FBP (1.6 ± 0.7) and ASIR (1.8 ± 0.7) ($p < 0.001$). There were no differences between the two readers in terms of the trend in subjective scoring with a matching order of ranking at all four image levels assessed. The overall difference between the pooled quality scores for ultralow-dose MBIR and standard-dose FBP was less than one half of 1 point (Table 3). The difference in quality scores between these two series was even smaller for the coronal assessments, indicating relative improvement in subjective image quality for the coronal versus transverse MBIR images (Fig. 3). With a threshold score of 3.0 or greater for acceptable image quality, in all but on case at least one subjective score between the two readers changed from unacceptable for both low-dose FBP and ASIR to acceptable for low-dose MBIR (97.8% [44/45]).

The pooled results of the blinded random review of the ultralow-dose image series for focal lesion detection are summarized in Table 4 and Figure 4C. With standard-dose FBP as the reference standard, significantly more noncalcific lesions were found on ultralow-dose MBIR images (79.3% [169/213], pooled) compared with ultralow-dose FBP (66.2% [141/213]) and ASIR (62.0% [132/213]) images ($p < 0.05$). The overall lesion detection rate with all three ultralow-dose reconstructions was significantly lower than the lesion detection rate with standard-dose FBP ($p < 0.05$). Although the number of focal lesions detected differed somewhat between the two readers, there was no significant difference in the relative performance for each dose and reconstruction type. Both readers detected fewer lesions on low-dose ASIR compared with low-dose FBP images, but the difference was not statistically significant. As expected, significantly fewer focal lesions were identified on the 24 sets of unenhanced images compared with the 21 sets of IV contrast-enhanced images (Table 6). Most of the focal lesions were small foci of low attenuation relative to the involved organ.

Discussion

The overarching goal of our ongoing prospective trial is to ultimately validate the use of ultralow-dose abdominal CT through the use of novel iterative reconstruction algorithms. This interim analysis provides the necessary data to determine whether our initially aggressive dose reduction goal should be modified. One important advantage of our prospective study design is the acquisition of the matching ultralow-dose series immediately after the standard-dose clinical series. This step allows not only direct side-by-side comparison of image noise and image quality but also assessment of diagnostic accuracy, for which it is critical to maintain an acceptable level of performance. Such comparison becomes less reliable when CT images obtained at different points in time are compared, as in most retrospective studies to date, or when simulated low-dose cases are used whereby noise is artificially introduced onto the images.

To our knowledge, this investigation is the first to use the FDA-approved commercial version of MBIR (Veo). Our preliminary findings show that MBIR is a substantial improvement over ASIR and FBP in terms of image noise, subjective image quality, and diagnostic performance. Interestingly, although ASIR had a modest incremental benefit over traditional FBP in terms of image noise and subjective image quality, the diagnostic performance of ASIR at the ultralow dose trended slightly poorer than that of low-dose FBP in terms of focal lesion detection and much poorer than that of MBIR. It should be noted, however, that ASIR is generally not intended for the aggressive dose reduction levels attained in this trial.

The interesting and important discordance between image quality measures and focal lesion detection seen for ASIR and FBP reconstructed images in this preliminary investigation was an unexpected finding that to our knowledge has not been previously reported and may be related to the aggressive levels of dose reduction in this study. This discordance also applies to the comparison between low-dose MBIR and the clinical reference standard of routine-dose FBP. The former had lower image noise but depicted fewer focal lesions overall. Clearly, image noise and subjective quality measurements alone are insufficient for validating novel ultralow-dose iterative reconstruction techniques. Additional objective quality metrics likely need to be developed and validated to better evaluate iterative reconstruction techniques. Beyond these quality evaluation metrics, it is critical to also assess lesion detection capability, which is a more direct assessment of diagnostic adequacy. As we accrue more patients in this ongoing prospective trial, we will eventually be able to assess closer-to-uniform discrete cohorts according to specific clinical indication and imaging technique.

As seen in the provided figures, the qualitative differences between MBIR and the other reconstruction techniques are readily apparent at very low doses. However, given that lesion detection was still compromised somewhat with ultralow-dose MBIR relative to standard-dose FBP, careful consideration is required in terms of defining the proper balance between dose reduction and diagnostic performance. Future investigations will focus more closely on diagnostic accuracy according to specific study indications, such as IV contrast-enhanced studies for oncologic follow-up, urolithiasis evaluation, and colorectal cancer screening. This interim analysis was neither powered nor intended to tackle these specific issues. Rather, by pooling the blinded detection of organ-based focal soft-tissue lesions in a more generic sense, we gain early insight into diagnostic performance. However, although clear trends were noted in terms of focal lesion detection, we must refrain from drawing firm conclusions with regard to diagnostic performance at this early point in the trial.

A number of recent studies have investigated the use of ASIR (ASiR, GE Healthcare), typically in a 30–40% blend with FBP [3–6], for achieving more modest dose reduction in the range of 25–40% on average. Similar studies have investigated a variety of other vendor-specific iterative reconstruction methods, such as iDose (Philips Healthcare) [14], iterative reconstruction in image space (IRIS, Siemens Healthcare) [15], and adaptive iterative dose reduction (AIDR, Toshiba) [16]. In general, the results of these studies all suggest or show a modest incremental benefit in terms of dose reduction, typically on the order of approximately 30%. However, most studies have largely been focused on noise reduction and subjective image quality, and diagnostic performance has not been directly assessed. At dose reduction levels approaching 90%, well beyond the usual indicated range for ASIR, our preliminary findings suggest that ASIR appears to be inadequate. This may also be the case for other vendor-specific algorithms that are not truly model based. Further investigation for these algorithms (ASiR, iDose, IRIS, AIDR) is needed to determine the radiation dose reduction levels at which diagnostic adequacy can be maintained relative to the current clinical reference standard in terms of lesion detection capability.

Despite the advantages of MBIR over ASIR and FBP found in our study, it is important to consider the current potential limitations. In addition to being vendor specific and requiring the raw projection data, the primary disadvantage of MBIR at this time lies in the demanding computational requirements, which lead to a prolonged reconstruction time. In the current study, the typical reconstruction time for a low-dose MBIR abdominal CT series was on the order of hours. As part of our prospective ultralow-dose clinical trial, we are assessing other novel iterative reconstruction techniques. One such method, prior image constrained compressed sensing (PICCS) [9, 17], may approach MBIR in terms of diagnostic quality but has the advantages of a reconstruction time that is approximately two orders of magnitude faster, can be used with DICOM image data, and is currently vendor neutral. As such, PICCS could service multiple scanners from different vendors within a department or group. At this time, however, use of the technique for dose reduction has not been fully clinically evaluated, nor is it commercially available.

The need for further lowering of dose levels for body CT is clear, regardless of whether this reaction is to a real or to a perceived health threat [1, 2, 18, 19]. In some ways, CT is a victim of its own clinical success; the sheer number of studies performed in the United States has increased from approximately 13 million in 1990 to approximately 46 and 67 million studies by 2000 and 2010 [20, 21]. The results of our preliminary work suggest that submillisievert abdominal CT is feasible for indications that call for unenhanced imaging. For standard IV contrast-enhanced abdominal CT, it appears that most examinations can be accomplished with effective doses well below 5 mSv, with the exception of imaging of some obese individuals. It is noteworthy that our patient population is generally overweight, a substantial fraction qualifying as obese. However, more work is needed to validate and refine the appropriate levels of dose reduction for contrast-enhanced CT that maintain an acceptable level of diagnostic accuracy. On the basis of our preliminary findings, our current thinking is to maintain the higher levels of dose reduction (80–90%) for unenhanced CT indications but to back off slightly to approximately 60–70% of the standard dose for IV contrast-enhanced studies.

We acknowledge a number of limitations to this study. This study was an interim analysis of an ongoing prospective trial and was not intended to resolve any indication-specific issues. Given the small sample size and heterogeneous techniques applied to this preliminary cohort, we would caution against any firm conclusions regarding the accuracy of ultralow-dose abdominal CT, especially because lesion-specific matching was not included. Furthermore, we did not address the possibility of pseudolesions (false-positive findings) among focal lesions detected at the ultralow dose. Larger homogeneous patient cohorts that

group common indications and study techniques are needed to better assess focal lesion detection and diagnostic accuracy. We intentionally kept the handling of focal lesion detection fairly generic for this initial report and allowed pooling of the data. Lesion characterization and clinical relevance were also not considered for this first analysis. We did not specifically address whether spatial resolution is preserved with the various reconstruction methods at ultralow doses, but we do intend to investigate this issue using a phantom. We did not investigate the use of dualenergy or low-kilovoltage imaging, nor did we acquire the ultralow-dose series in the arterial or more delayed phases of contrast enhancement. These issues can be addressed at a later date as part of the ongoing prospective trial. Finally, the percentage dose reduction relative to standard in our study was lessened by the use of the ASIR-driven protocols and would have been greater if the older FBP protocols had been used.

In summary, MBIR shows great promise for substantially reducing radiation doses at abdominal CT in clinical practice, whereas ASIR and FBP appear to be of limited value for the aggressive radiation dose levels targeted in this study. Further investigation is needed to determine the optimal indication-specific dose levels that maintain adequate diagnostic performance with MBIR. An important finding was that objective and subjective image quality measures do not necessarily correlate with diagnostic performance at ultralow-dose CT.

Acknowledgments

Supported in part by grant 1R01 CA169331-01 from the National Institutes of Health–National Cancer Center.

References

1. Brenner DJ, Hall EJ. Computed tomography: an increasing source of radiation exposure. *N Engl J Med*. 2007; 357:2277–2284. [PubMed: 18046031]
2. Pearce MS, Salotti JA, Little MP, et al. Radiation exposure from CT scans in childhood and subsequent risk of leukaemia and brain tumours: a retrospective cohort study. *Lancet*. 2012; 380:499–505. [PubMed: 22681860]
3. Singh S, Kalra MK, Hsieh JA, et al. Abdominal CT: comparison of adaptive statistical iterative and filtered back projection reconstruction techniques. *Radiology*. 2010; 257:373–383. [PubMed: 20829535]
4. Sagara Y, Hara AK, Pavlicek W, et al. Comparison of low-dose CT with adaptive statistical iterative reconstruction and routine-dose CT with filtered back projection in 53 Patients. *AJR*. 2010; 195:713–719. [PubMed: 20729451]
5. Flicek KT, Hara AK, Silva AC, Wu Q, Peter MB, Johnson CD. Reducing the radiation dose for CT colonography using adaptive statistical iterative reconstruction: a pilot study. *AJR*. 2010; 195:126–131. [PubMed: 20566805]
6. Prakash P, Kalra MK, Kambadakone AK, et al. Reducing abdominal CT radiation dose with adaptive statistical iterative reconstruction technique. *Invest Radiol*. 2010; 45:202–210. [PubMed: 20177389]
7. Hara AK, Paden RG, Silva AC, Kujak JL, Lawder HJ, Pavlicek W. Iterative reconstruction technique for reducing body radiation dose at CT: feasibility study. *AJR*. 2009; 193:764–771. [PubMed: 19696291]
8. Kambadakone AR, Chaudhary NA, Desai GS, Nguyen DD, Kulkarni NM, Sahani DV. Low-dose MDCT and CT enterography of patients with Crohn disease: feasibility of adaptive statistical iterative reconstruction. *AJR*. 2011; 196:1340. [web]W743–W752.
9. Lubner MG, Pickhardt PJ, Tang J, Chen GH. Reduced image noise at low-dose multidetector CT of the abdomen with prior image constrained compressed sensing algorithm. *Radiology*. 2011; 260:248–256. [PubMed: 21436086]

10. Mitsumori LM, Shuman WP, Busey JM, Kolokythas O, Koprowicz KM. Adaptive statistical iterative reconstruction versus filtered back projection in the same patient: 64 channel liver CT image quality and patient radiation dose. *Eur Radiol.* 2012; 22:138–143. [PubMed: 21688003]
11. Marin D, Nelson RC, Rubin GD, Schindera ST. Body CT: technical advances for improving safety. *AJR.* 2011; 197:33–41. [PubMed: 21701008]
12. McCollough, C.; Cody, D.; Edyvean, S., et al. The measurement, reporting and management of radiation dose in CT. College Park, MD: AAPM; 2008. American Association of Physicists in Medicine (AAPM). Report no. 96
13. Deak PD, Smal Y, Kalender WA. Multisection CT protocols: sex- and age-specific conversion factors used to determine effective dose from doselength product. *Radiology.* 2010; 257:158–166. [PubMed: 20851940]
14. Noël PB, Fingerle AA, Renger B, Münzel D, Rummeny EJ, Dobritz M. Initial performance characterization of a clinical noise-suppressing reconstruction algorithm for MDCT. *AJR.* 2011; 197:1404–1409. [PubMed: 22109296]
15. Lee SJ, Park SH, Kim AY, et al. A prospective comparison of standard-dose CT enterography and 50% reduced-dose CT enterography with and without noise reduction for evaluating Crohn disease. *AJR.* 2011; 197:50–57. [PubMed: 21701010]
16. Gervaise A, Osemont B, Lecocq S, et al. CT image quality improvement using adaptive iterative dose reduction with wide-volume acquisition on 320-detector CT. *Eur Radiol.* 2012; 22:295–301. [PubMed: 21927791]
17. Chen GH, Tang J, Leng S. Prior image constrained compressed sensing (PICCS): a method to accurately reconstruct dynamic CT images from highly undersampled data sets. *Med Phys.* 2008; 35:660–663. [PubMed: 18383687]
18. Health Physics Society Website. Radiation risk in perspective: position statement of the Health Physics Society. https://documents/risk_ps010-2.pdf. Published January 1996. Updated July 2010. Accessed July 27, 2012
19. Brenner DJ, Georgsson MA. Mass screening with CT colonography: should the radiation exposure be of concern? *Gastroenterology.* 2005; 129:328–337. [PubMed: 16012958]
20. Mahesh M. NCRP report number 160: its significance to medical imaging. *J Am Coll Radiol.* 2009; 6:890–892. [PubMed: 19945048]
21. Ionizing radiation exposure of the population of the United States. Bethesda, MD: NCRP; 1987. National Council on Radiation Protection and Measurements. Report no. 93

APPENDIX I

Abdominal MDCT Standard-Dose Protocols Used in the Prospective Trial

| Parameter | Protocol | | |
|---|---------------------------------|---------------------------------|---------------------------------|
| | IV Contrast Enhanced | Urolithiasis | Supine CT Colonography |
| Scanner | Discovery CT750 HD ^a | Discovery CT750 HD ^a | Discovery CT750 HD ^a |
| Scan type | Helical | Helical | Helical |
| Rotation time (s) | 0.5 | 0.8 | 0.5 |
| Beam collimation (mm) | 40 | 40 | 40 |
| No. of detector rows | 64 | 64 | 64 |
| Pitch | 0.516 | 0.516 | 0.984 |
| Speed (mm/rotation) | 20.64 | 20.64 | 39.36 |
| Detector configuration | 64 × 0.625 | 64 × 0.625 | 64 × 0.625 |
| Slice thickness for noise index (mm) | 1.25 | 1.25 | 1.25 |
| Scan FOV | Large body | Large body | Large body |
| Peak kilovoltage | 120 | 120 | 120 |
| Smart mA (GE Healthcare) range (mA) | 60–660 | 40–660 | 30–300 |
| Noise index | 24 | 28 | 50 |
| Reconstruction (filtered back projection) | | | |
| Displayed FOV (cm) | 36–50 | 36–50 | 36–50 |
| Reconstruction type | Standard | Standard | Standard |
| Window width/level (HU) | 400/50 | 400/50 | 400/50 |
| Reconstruction option | Plus | Plus | Plus |
| Slice thickness (mm) | 2.5 | 2.5 | 2.5 |
| Interval (mm) | 1.5 | 1.5 | 1.5 |

Note—The protocols considered standard dose in this study are based on use of 40% adaptive statistical iterative reconstruction, which affects the relative dose reduction seen at low dose. The specific protocol for the accompanying low-dose series was derived by adjusting the noise index–slice thickness pairing (and tube current range) to allow targeted 70–90% dose reduction (by projected dose-length product) relative to the standard-dose series.

^aGE Healthcare.

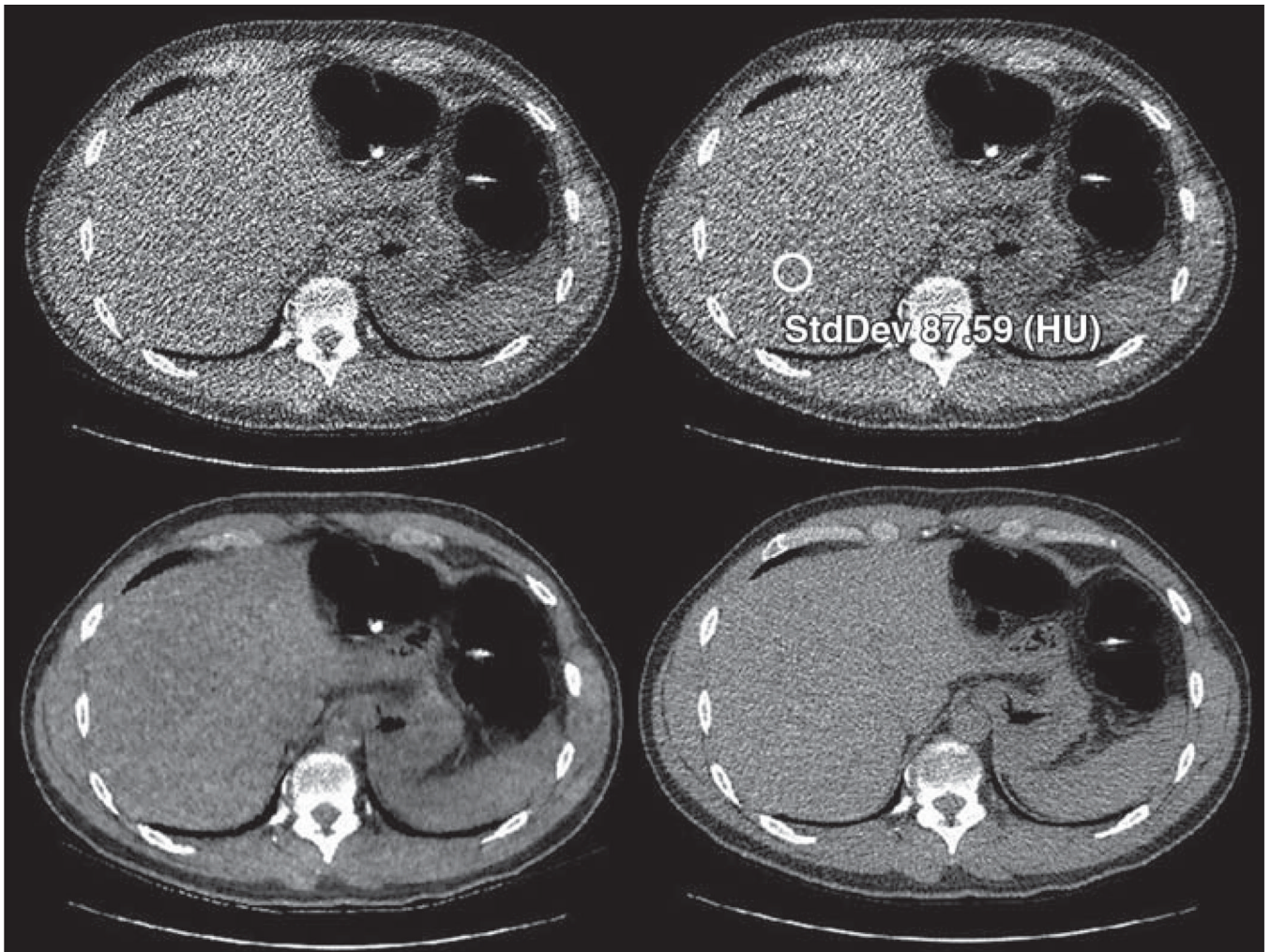


Fig. 1. 42-year-old man (body mass index, 24.4) who underwent unenhanced abdominal MDCT colonography. Low-dose reconstructions include filtered back projection (FBP) (*top left*), adaptive statistical iterative reconstruction (ASIR) (*top right*), and model-based iterative reconstruction (MBIR) (*bottom left*). Effective dose for low-dose series was 0.35 mSv, representing 87% dose reduction relative to standard-dose FBP series (*bottom right*). Region-of-interest placement in right hepatic lobe (*circle*) for image noise measurement is shown on ASIR image.

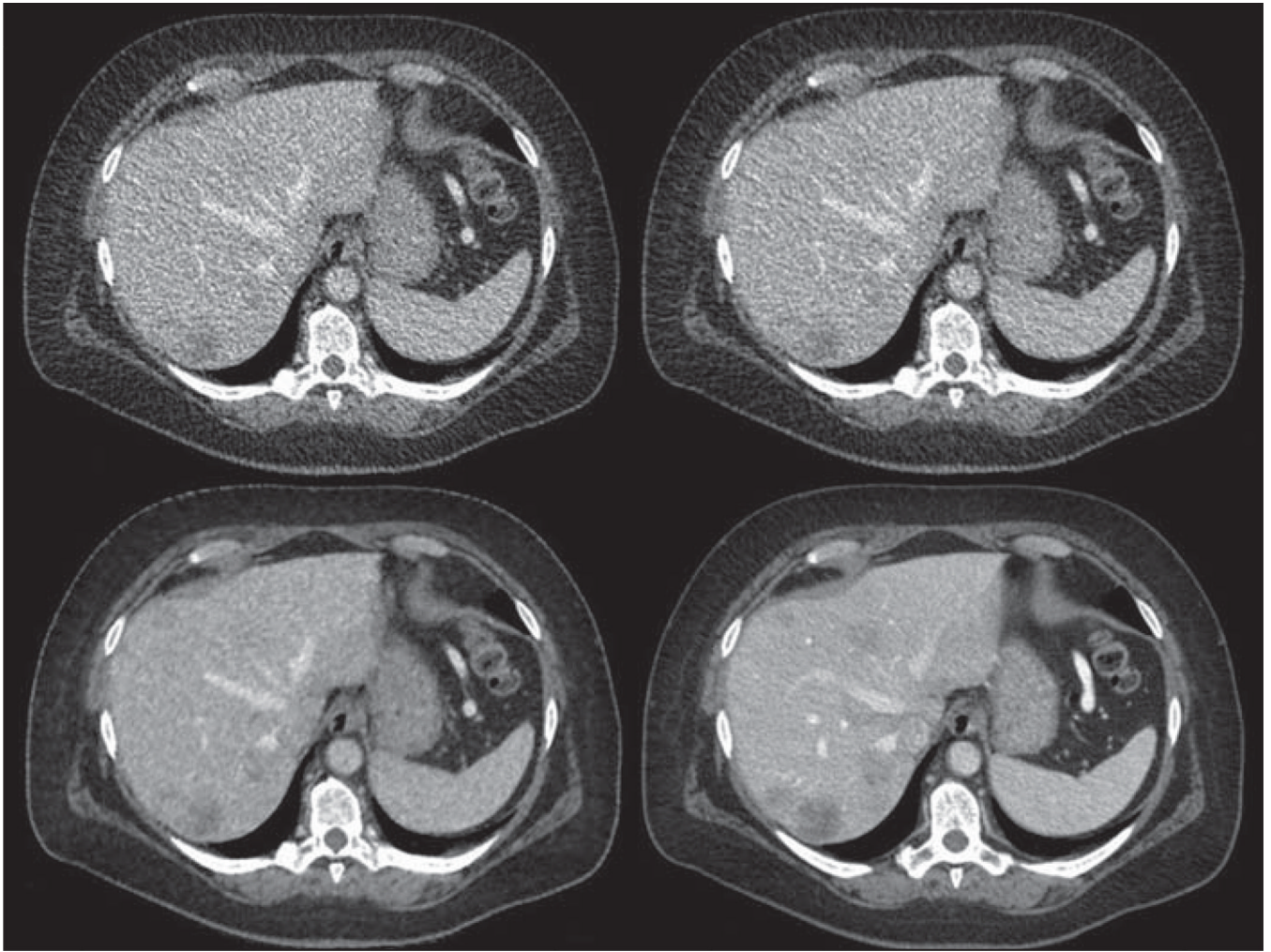


Fig. 2. 55-year-old woman (body mass index, 39.8) with treated liver metastasis from pancreatic endocrine tumor who underwent contrast-enhanced abdominal MDCT. Effective dose for low-dose series (filtered back projection [FBP] [*top left*], adaptive statistical iterative reconstruction [ASIR] [*top right*], and model-based iterative reconstruction (MBIR) [*bottom left*]) was 2.3 mSv, representing 88% reduction relative to standard-dose FBP series (*bottom right*). One reader detected only four low-attenuation liver lesions on low-dose ASIR images but identified at least seven focal liver lesions (per-organ maximum) on other images.

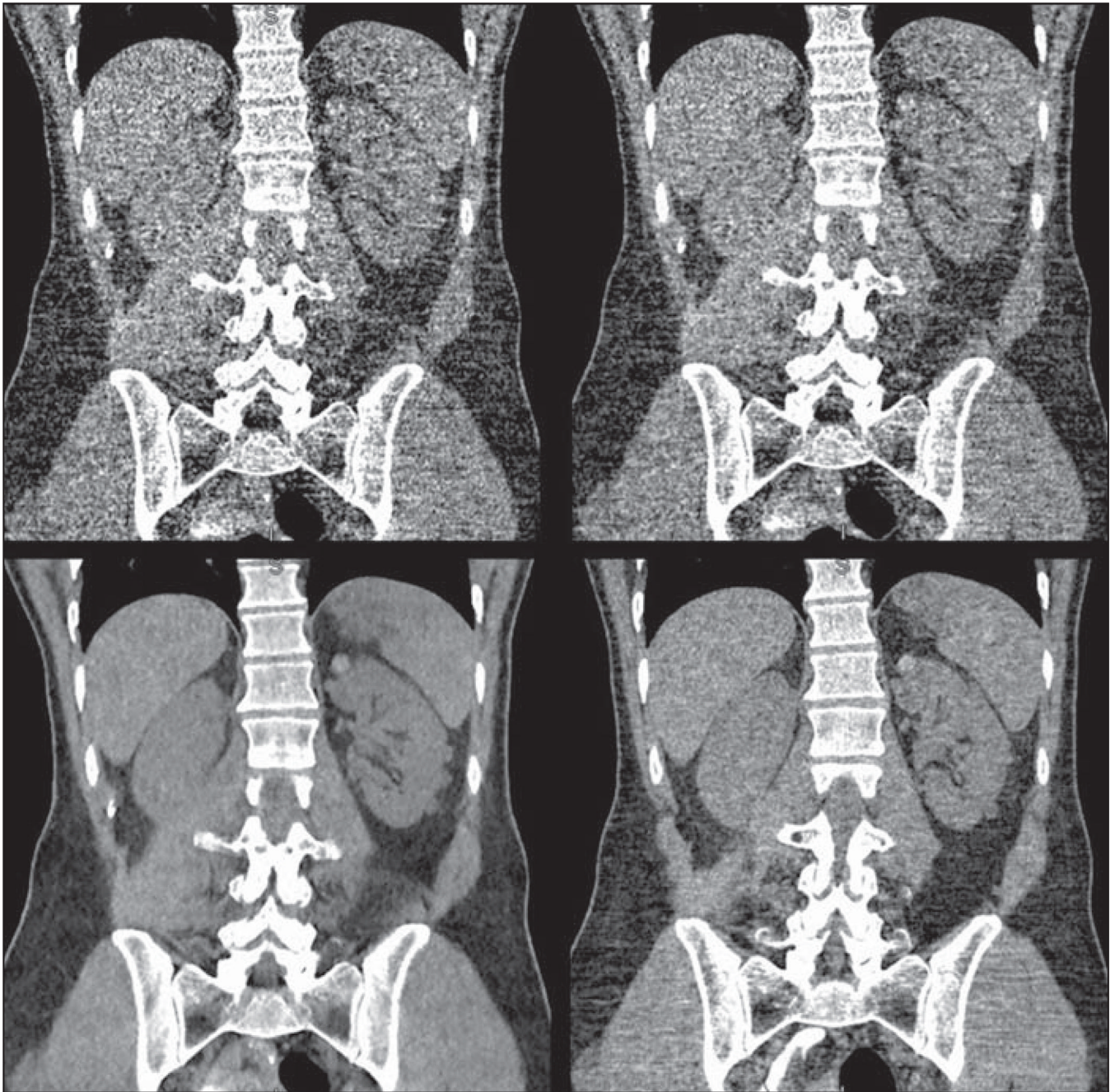
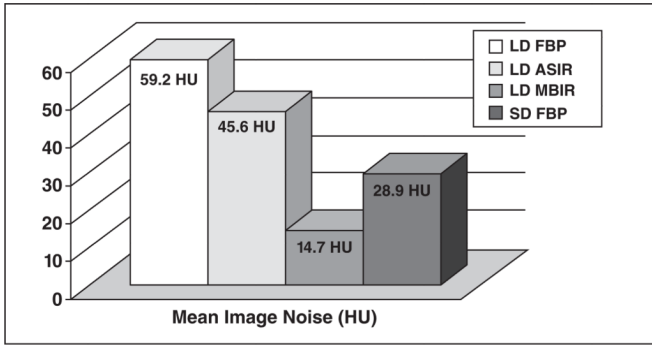
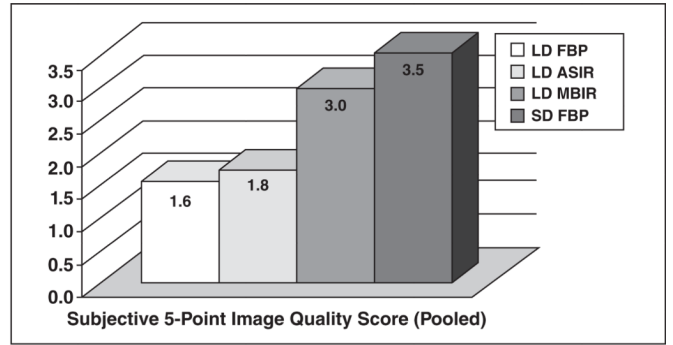


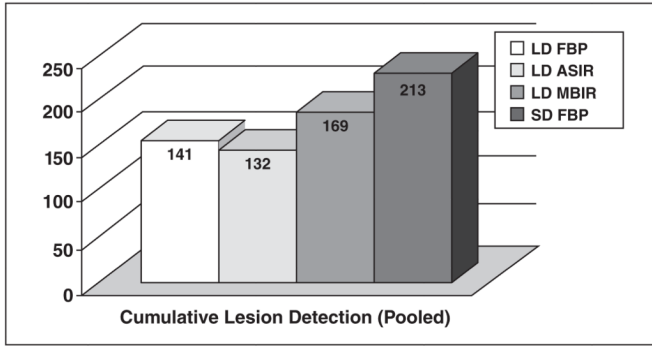
Fig. 3. 59-year-old man (body mass index, 23.7) with renal lesions. Coronal reconstructions from unenhanced abdominal MDCT through level of kidneys. Effective dose for low-dose series (filtered back projection [FBP] [*top left*], adaptive statistical iterative reconstruction [ASIR] [*top right*], and model-based iterative reconstruction [MBIR] [*bottom left*]) was 0.35 mSv, 79% reduction relative to standard dose (*bottom right*). Both readers identified per-organ maximum number of soft-tissue lesions (7) in left kidney on both standard-dose FBP and low-dose MBIR images but called 11 lesions combined on low-dose FBP image and only four lesions combined on ASIR image. Low-dose MBIR image rivals or even surpasses image quality of standard-dose FBP image.



A



B



C

Fig. 4. Overall pooled results. A–C, Bar graphs show overall pooled results for image noise (A), subjective image quality (B), and lesion detection (C) for each reconstruction. LD = low-dose, FBP = filtered back projection, ASIR = adaptive statistical iterative reconstruction, MBIR = model-based iterative reconstruction, SD = standard dose.

TABLE 1

Patient-Specific Data Regarding Demographics and Abdominal CT Dose

| Patient No. | Age (y) | Sex | BMI | IV Contrast Material Administered | CTDI _{vol} (mGy) | | Dose Reduction From Standard (%) |
|-------------|---------|-----|------|-----------------------------------|---------------------------|-----------------|----------------------------------|
| | | | | | Standard-Dose Series | Low-Dose Series | |
| 1 | 71 | M | 38.2 | No | 10.88 | 2.76 | 75 |
| 2 | 42 | M | 24.4 | No | 3.63 | 0.48 | 87 |
| 3 | 56 | F | 21.6 | No | 1.43 | 0.40 | 72 |
| 4 | 71 | F | 30.4 | No | 3.68 | 0.79 | 79 |
| 5 | 62 | F | 34.9 | No | 5.88 | 1.23 | 79 |
| 6 | 50 | F | 31.3 | No | 6.20 | 1.32 | 79 |
| 7 | 52 | M | 24.8 | No | 2.03 | 0.44 | 78 |
| 8 | 51 | F | 24.0 | No | 2.47 | 0.59 | 76 |
| 9 | 59 | M | 23.7 | No | 2.23 | 0.48 | 78 |
| 10 | 55 | M | 31.3 | No | 4.09 | 0.85 | 79 |
| 11 | 86 | F | 28.1 | No | 10.31 | 1.42 | 86 |
| 12 | 42 | M | 25.7 | No | 6.67 | 1.50 | 78 |
| 13 | 28 | M | 26.1 | No | 8.05 | 1.50 | 81 |
| 14 | 58 | F | 26.4 | No | 7.31 | 1.58 | 78 |
| 15 | 80 | M | 25.5 | No | 7.95 | 1.50 | 81 |
| 16 | 71 | M | 31.5 | No | 16.60 | 2.66 | 84 |
| 17 | 29 | M | 27.7 | No | 9.80 | 1.53 | 84 |
| 18 | 62 | M | 20.8 | No | 5.97 | 1.52 | 75 |
| 19 | 59 | F | 34.2 | No | 12.87 | 2.04 | 84 |
| 20 | 43 | F | 26.5 | No | 7.50 | 1.39 | 81 |
| 21 | 63 | F | 38.8 | Yes | 21.26 | 8.48 | 60 |
| 22 | 35 | F | 23.1 | Yes | 4.54 | 1.29 | 72 |
| 23 | 77 | F | 24.0 | Yes | 4.85 | 1.53 | 68 |
| 24 | 48 | M | 26.1 | Yes | 14.33 | 5.66 | 61 |
| 25 | 72 | F | 35.9 | Yes | 25.71 | 10.25 | 60 |
| 26 | 82 | M | 28.4 | Yes | 14.51 | 3.78 | 74 |
| 27 | 55 | F | 39.8 | Yes | 32.09 | 3.94 | 88 |

| Patient No. | Age (y) | Sex | BMI | IV Contrast Material Administered | CTDI _{vol} (mGy) | | Dose Reduction From Standard (%) |
|-------------|---------|-----------|------|-----------------------------------|---------------------------|-----------------|----------------------------------|
| | | | | | Standard-Dose Series | Low-Dose Series | |
| 28 | 85 | F | 33.8 | Yes | 35.30 | 15.05 | 57 |
| 29 | 57 | M | 41.6 | Yes | 79.83 | 26.45 | 67 |
| 30 | 41 | F | 24.3 | No | 7.72 | 1.48 | 81 |
| 31 | 66 | M | 26.1 | No | 10.06 | 1.60 | 84 |
| 32 | 77 | F | 30.1 | Yes | 11.69 | 4.55 | 61 |
| 33 | 41 | M | 28.8 | Yes | 7.85 | 1.47 | 81 |
| 34 | 63 | M | 35.1 | Yes | 19.55 | 7.71 | 61 |
| 35 | 79 | M | 24.4 | No | 7.35 | 2.88 | 61 |
| 36 | 39 | M | 21.6 | Yes | 5.39 | 1.98 | 63 |
| 37 | 58 | F | 19.4 | Yes | 4.56 | 1.09 | 76 |
| 38 | 42 | M | 28.1 | Yes | 11.59 | 4.56 | 61 |
| 39 | 60 | F | 23.6 | Yes | 5.92 | 2.16 | 64 |
| 40 | 48 | M | 24.3 | Yes | 7.29 | 2.88 | 60 |
| 41 | 76 | M | 27.9 | Yes | 41.48 | 10.08 | 76 |
| 42 | 50 | F | 33.0 | No | 6.17 | 1.31 | 79 |
| 43 | 52 | F | 30.3 | Yes | 17.88 | 3.23 | 82 |
| 44 | 42 | M | 32.4 | Yes | 34.22 | 4.14 | 88 |
| 45 | 69 | M | 25.9 | Yes | 7.10 | 2.77 | 61 |
| Mean | 57.9 | 24 M, 21F | 28.5 | | 12.75 | 3.47 | 74 |

Note—BMI = body mass index, CTDI_{vol} = volume CT dose index.

TABLE 2

Mean Image Noise According to Dose and Reconstruction Method

| Site | With IV Contrast Enhancement (n = 21) | | | | Without IV Contrast Enhancement (n = 24) | | | | Entire Cohort (n = 45) | | | | | |
|--------|---------------------------------------|---------------|-------------------|---------------|--|---------------|-------------------|---------------|------------------------|---------------|-------------------|---------------|---------------|-------------------|
| | Low-Dose FBP | Low-Dose MBIR | Standard-Dose FBP | Low-Dose ASIR | Low-Dose FBP | Low-Dose MBIR | Standard-Dose FBP | Low-Dose ASIR | Low-Dose FBP | Low-Dose MBIR | Standard-Dose FBP | Low-Dose ASIR | Low-Dose MBIR | Standard-Dose FBP |
| Liver | 44.5 | 48.5 | 14.1 | 23.8 | 79.4 | 60.3 | 16.3 | 33.9 | 63.1 | 48.3 | 15.3 | 29.2 | | |
| Kidney | 44.9 | 35.0 | 16.0 | 26.7 | 73.0 | 55.9 | 14.4 | 33.7 | 59.8 | 46.1 | 15.1 | 30.4 | | |
| Fat | 38.7 | 30.0 | 11.4 | 21.7 | 69.1 | 53.7 | 14.6 | 30.3 | 54.9 | 42.6 | 13.1 | 26.3 | | |
| Muscle | 42.7 | 33.1 | 15.3 | 25.4 | 73.0 | 55.8 | 15.5 | 33.3 | 58.8 | 45.2 | 15.4 | 29.6 | | |
| Total | 42.7 | 36.7 | 14.2 | 24.4 | 73.6 | 56.4 | 15.2 | 32.8 | 59.2 | 45.6 | 14.7 | 28.9 | | |

Note—All measurements are in HU. Image noise refers to the SD around the mean region-of-interest attenuation measurement. FBP = filtered back-projection, ASIR = adaptive statistical iterative reconstruction, MBIR = model-based iterative reconstruction.

TABLE 3
 Mean Subjective Image Quality Scores in 45 Cases According to Dose and Reconstruction Method

| Level | Reader 1 | | | | Reader 2 | | | | Pooled Results | | | |
|-------------------|-----------------|------------------|------------------|----------------------|-----------------|------------------|------------------|----------------------|-----------------|------------------|------------------|----------------------|
| | Low-Dose FBP | Low-Dose ASIR | Low-Dose MBIR | Standard-Dose FBP | Low-Dose FBP | Low-Dose ASIR | Low-Dose MBIR | Standard-Dose FBP | Low-Dose FBP | Low-Dose ASIR | Low-Dose MBIR | Standard-Dose FBP |
| Axial | | | | | | | | | | | | |
| Main portal vein | 1.1 | 1.5 | 2.6 | 3.2 | 1.6 | 1.8 | 2.9 | 3.6 | 1.4 | 1.6 | 2.7 | 3.4 |
| Sacroiliac joints | 1.2 | 1.6 | 2.6 | 3.2 | 2.3 | 2.4 | 3.3 | 3.9 | 1.7 | 2.0 | 3.3 | 3.9 |
| Coronal | | | | | | | | | | | | |
| Kidney | 1.4 | 1.7 | 3.1 | 3.3 | 2.2 | 2.3 | 3.4 | 3.8 | 1.8 | 2.0 | 3.2 | 3.6 |
| Main portal vein | 1.0 | 1.4 | 2.9 | 3.2 | 1.9 | 2.0 | 3.2 | 3.6 | 1.4 | 1.7 | 3.0 | 3.4 |
| Total | 1.2 | 1.6 | 2.8 | 3.2 | 2.0 | 2.1 | 3.2 | 3.7 | 1.6 | 1.8 | 3.0 | 3.5 |

Note—Subjective image quality was based on blinded review and assessed with a 5-point scoring system (0–4 points) based on that proposed by Flicek et al. [5]. FBP = filtered back projection, ASIR = adaptive statistical iterative reconstruction, MBIR = model-based iterative reconstruction.

TABLE 4
 Cumulative Focal Lesion Detection in 45 Cases According to Dose and Reconstruction Method

| Location | Reader 1 | | | | Reader 2 | | | | Pooled Results | | | | | | | |
|--------------|-----------------|------------------|------------------|----------------------|-----------------|------------------|------------------|----------------------|-----------------|------------------|------------------|----------------------|-----------------|------------------|------------------|----------------------|
| | Low-Dose FBP | Low-Dose ASiR | Low-Dose MBiR | Standard-Dose FBP |
| Liver | 26 | 23 | 27 | 41 | 26 | 26 | 33 | 49 | 52 | 49 | 60 | 90 | 52 | 49 | 60 | 90 |
| Pancreas | 3 | 3 | 3 | 3 | 4 | 4 | 5 | 5 | 7 | 7 | 8 | 8 | 7 | 7 | 8 | 8 |
| Right kidney | 13 | 14 | 18 | 19 | 15 | 11 | 16 | 17 | 28 | 25 | 34 | 36 | 28 | 25 | 34 | 36 |
| Left kidney | 32 | 28 | 34 | 41 | 22 | 23 | 33 | 38 | 54 | 51 | 67 | 79 | 54 | 51 | 67 | 79 |
| Total | 74 | 68 | 82 | 104 | 67 | 64 | 87 | 109 | 141 | 132 | 169 | 213 | 141 | 132 | 169 | 213 |

Note—FBP = filtered back-projection, ASiR = adaptive statistical iterative reconstruction, MBiR = model-based iterative reconstruction.

TABLE 5

Lesion Detection According to CT Study Type (Unenhanced vs Contrast-Enhanced)

| CT Study Type | Focal Lesions (Pooled) | | | |
|--------------------------------|------------------------|---------------|---------------|-------------------|
| | Low-Dose FBP | Low-Dose ASIR | Low-Dose MBIR | Standard-Dose FBP |
| Unenhanced ($n = 24$) | 16 | 10 | 24 | 37 |
| Contrast-enhanced ($n = 22$) | 125 | 122 | 145 | 176 |
| All studies ($n = 45$) | 141 | 132 | 169 | 213 |

Note—FBP = filtered back-projection, ASIR = adaptive statistical iterative reconstruction, MBIR = model-based iterative reconstruction.